Title	A preliminary investigation on face recognition as a biometric identifier of sheep
Authors(s)	Corkery, Gerard; Gonzales-Barron, Ursula A.; Butler, Francis; McDonnell, Kevin; Ward, Shane
Publication date	2007
Publication information	Transactions of the ASABE, 50 (1): 313-320
Publisher	The American Society of Agricultural and Biological Engineers
Link to online version	http://elibrary.asabe.org/abstract.asp?aid=22395&redir=[volume=50&issue=1&conf=t&orgconf=]&r
Item record/more information	http://hdl.handle.net/10197/4294

A PRELIMINARY INVESTIGATION ON FACE RECOGNITION AS A BIOMETRIC IDENTIFIER OF SHEEP

G. P. Corkery, U. A. Gonzales-Barron, F. Butler, K. Mc Donnell, S. Ward

ABSTRACT. *The suitability of face recognition was investigated as a biometric-based identifier for sheep using a holistic analysis of face images by the independent components technique. Algorithm training was performed independently on several normalized face images from 50 sheep (sets of two, three, and four training images per sheep). The performance of this technique was assessed on a separate set of images (three normalized face images per sheep) using the cosine distance classifier. When 180 to 200 components were extracted, the recognition rate was as high as 95.3% to 96%. As expected, fewer independent components reduced the recognition rate, while a higher number of training images per sheep improved it. Although our results have demonstrated the potential of face recognition as a non-invasive, inexpensive, and accurate novel biometric identifier of sheep, further work should aim at improving recognition rates on a larger set of sheep faces.*

Keywords. *Biometrics, Face recognition, Identification, Sheep, Traceability*.

Major disease outbreaks such as bovine spongiform encephalopathy (BSE), foot and mouth disease (FMD), and swine fever, along with the importance of export markets for national producers, have prompted the implementation of animal identification and verification programs internationally. Traceability refers to the ability to identify farm animals and their products according to their origin, as far back in the production sequence as is necessary to ascertain ownership, identify parentage, ensure food safety, and ensure compliance (e.g., for source verification, process verification, production practice verification, beef export verification, and authenticity management). In Ireland, the National Sheep Identification System (NSIS), which came into effect in June 2001, involves the individual identification of all sheep by ear tagging. However, any method of identification must not only be effective but must also safeguard the welfare of the animal. Edwards et al. (2001) showed that the insertion of ear tags normally results in an inflammatory response (and extreme discomfort and pain, especially if the ear is handled when reading the tag) and that ear tags could cause both short- and long-term complications to the integrity of the ears. After examination of the ears of over 700 sheep, Edwards and Johnston (1999) found that approximately 28% of the animals suffered slight to moderate ear damage associated with plastic ear tags, including local inflammation, pronounced thickening, traces of hemorrhaging, and mild sepsis. In their study, Edwards et al. (2001) also observed incidence of tag loss in lambs due to the tag tearing through the ear.

While an animal can be allocated an identification number and the system of identification is made tamper-proof as far as possible, it may be necessary to verify an animal's identity against an invariant parameter in situations where the identity of the animal is in doubt. This invariant parameter (1) must be fraud-proof; (2) must be based on a robust biometric marker (physical, anatomical, or biomolecular invariant trait that uniquely identifies a particular animal); (3) its acquisition must be rapid, inexpensive, and accurate; and (4) the acquisition method must be humane and non-invasive. As Dziuk (2003) pointed out, the presence of an effective verification system would also reduce the temptation to commit fraud and would reduce actual fraud. According to Rusk et al. (2006), only iris imaging, retinal scanning, and retinal imaging are potentially suitable as a secure biometric identification method for animals (other than humans). However, other means of identifying livestock through biometrics have been proposed by Smith et al. (2005), and they encompass DNA fingerprinting, autoimmune antibody matching, muzzle pattern matching, and facial recognition. Nevertheless, while considerable attention has been paid to animal DNA testing and bioactive labels (Loftus, 2005; Jiménez Gamero et al., 2006; Raschke et al., 2006), muzzle pattern recognition and facial recognition have been merely disregarded. In preparing this article, no peer-reviewed publications were found on facial recognition for livestock.

Facial images are the most common biometric characteristic used by humans to make a personal recognition, hence the interest in using this biometric. Face recognition is a non-intrusive method that can be made from still images, video sequences, stereo images, range images, or thermal images (de Luis García et al., 2003). The most popular approaches to face recognition are based mainly on either: (1) the location and shape of facial attributes such as eyes, eyebrows, nose, lips, and chin, and their spatial relationship;

Submitted for review in June 2006 as manuscript number IET 6519; approved for publication by the Information & Electrical Technologies Division of ASABE in December 2006.

The authors are **Gerard P. Corkery,** Graduate Student, **Ursula A. Gonzales-Barron,** Postdoctoral Researcher, **Francis Butler,** Senior Lecturer, **Kevin McDonnell,** Lecturer, and **Shane Ward,** Professor, Biosystems Engineering, School of Agriculture, Food Science and Veterinary Medicine, University College Dublin, Dublin, Ireland. **Corresponding author:** Ursula Gonzales-Barron, Biosystems Engineering, School of Agriculture, Food Science and Veterinary Medicine, University College Dublin, Earlsfort Terrace, Dublin 2, Ireland; phone: +353-1716-5589; fax: +353-1475-2119; ursula.gonzalesbarron@ucd.ie.

or (2) the overall analysis of the face image, using either holistic or subspace methods, that represents a face as a weighted combination of a number of source faces (Delac and Grgic, 2004). According to Shakhnarovich and Moghaddam (2004), the subspace methods have been shown to be highly successful in human face recognition, and in many other vision tasks, as they assume that complex phenomena such as images of human faces, represented in a high-dimensional measurement space, are often intrinsically low-dimensional. Thus, exploiting this low dimensionality would then allow a face recognition system to focus attention on the features of the data relevant for the identity of an individual.

Our particular interest in employing the independent component analysis (ICA) technique for face representation relies on two aspects: (1) ICA has been found to have a high invariance to changes in pose and illumination (Bartlett et al., 2002; Yuen and Lai, 2002), and (2) ICA subspace representation takes into account higher-order statistics, which are able to capture the phase spectrum (Bell and Sejnowski, 1997). The phase spectrum, not the power spectrum, contains the structural information in images that drives human perception. For example, a face image synthesized from the amplitude spectrum of face A and the phase spectrum of face B will be perceived as an image of face B. The fact that ICA is sensitive to the phase spectrum of images suggests that it might be particularly well suited for representing natural images (Bartlett et al., 2002). The objective of this work was to investigate the potential of facial recognition as a biometric-based identification system for sheep by using a subspace method based on the independent component analysis technique.

Materials and Methods

Image Acquisition and Normalization

Fifty sheep faces were imaged over a period of five weeks. The sheep (3 to 4 years old) were crossbreeds of Cheviot and Suffolk breeds. Each sheep was restrained in a holding pen. To reduce image variability due to the presence of external dirt, the sheep faces were gently cleaned with a soft brush. Digital images of the frontal face were taken at a distance of about 1 m using a digital still camera (PowerShot G3, Canon, Inc., Tokyo, Japan) at a resolution of 1024 × 768 pixels. Every week, 5 to 10 photos were acquired per individual sheep in order to capture an adequate pose, such as the one shown in figure 1a. The best photo was then selected in terms of face position, fraction of face area within the image, and focus. This selection process was entirely based on human observation. Four face images per sheep (200 images in total) were used for the training stage of the facial recognition algorithm (fig. 3), and another three face images per sheep (150 images in total) were used as test images for the verification stage.

The function of the independent component analysis (ICA) is to determine the underlying variations that cause some observable result, so ICA attempts to explain macroscopic, high-dimensional observations with low-dimensional variations. If we were to attempt face recognition on facial images that varied in scale, lighting, and rotation with no compensation for these variations, the dimensionality of the decomposition problem would grow dramatically, and as a result, ICA would fail at classifying the underlying trends because of the high dimensionality of the problem. For the ICA technique to work, our system must have some form of pre-processing algorithm that compensates for adjustments in scale, rotation, and lighting. Thus, the normalization stage transforms the facial image into a standard format that removes or attenuates variations that can affect recognition performance. Sheep faces were then normalized in the following four steps:

1. Rotation: Once images were converted to gray level, in-plane rotation was done by manually locating two facial key points, the center of the eyes.
2. Scaling and cropping: To adjust for horizontal scaling, the length of the left-right eye line was determined. Let this be termed the "horizontal span." By resizing the width of the image to some constant divided by the horizontal span (new width = 150 × 1024/horizontal span), the new length of the left-right eye line will become a constant. The process for vertical scale compensation is similar. In this case, the height of the image was set to some constant divided by the "vertical span" (new height = 180 × 768/vertical span). The vertical span was the distance between the center of the mouth and the eye line (Cendrillón, 1999). As a result, the center of the eyes and mouth were translated to approximately standard positions within a cropped image of 200 × 280 pixels.
3. Low-pass filtering: To remove high-frequency noise, the images were smoothed with a 3 × 3 Gaussian filter (González et al., 2004).
4. Illumination normalization: Since there was no control of lighting conditions when the images were acquired, it was necessary to attenuate illumination variation among images, as this is a critical factor in algorithm performance (Moon and Phillips, 2001). For this purpose, the gray level histogram of each image was equalized.

Figure 1a shows a sheep face image as acquired with the digital camera, and figure 1b shows the sheep face image after rotation, scaling, cropping, and filtering.

Independent Component Analysis

Independent component analysis is intimately related to the blind source separation (BSS) problem (Cardoso, 1997), where the goal is to decompose an observed signal into a linear combination of unknown independent signals. Let s be a vector of unknown source signals and x be a vector of observed mixtures. If A is an unknown mixing matrix, then the mixing model is written as:

$$x = As \tag{1}$$

It is assumed that the source signals are independent of each other and the mixing matrix A is invertible. Based on these assumptions and the observed mixtures, ICA algorithms try to find the mixing matrix A or the separating matrix W such that:

$$u = Wx = WAs \tag{2}$$

is an estimation of the independent source signals (fig. 2).

The whitening transform is applied to the observed mixtures to obtain a set of statistically independent signals.

Figure 1. (a) A raw image (1024 × 768 pixels) of a sheep face taken with a digital camera, and (b) the resulting image (200 × 280 pixels) after normalization.

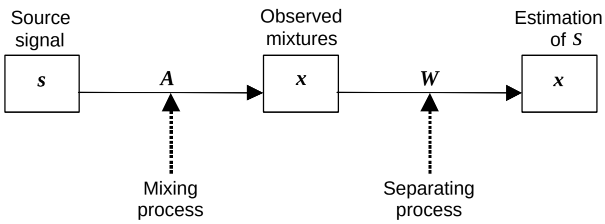

Figure 2. Blind source separation model.

Unfortunately, there may not be any matrix W that fully satisfies the independence condition, and there is no closed expression to find W. Instead, there are several algorithms that iteratively approximate W so as to indirectly maximize independence. Since it is difficult to maximize the independence condition directly, all common ICA algorithms recast the problem to iteratively optimize a smooth function whose global optima occurs when the output vectors u are independent. For instance, InfoMax relies on the observation that independence is maximized when the entropy $H(u)$ is maximized (eq. 5).

Statistically Independent Basis Images

The approach of independent component analysis used in this work was the architecture of statistically independent basis images presented by Bartlett et al. (2002) based on the InfoMax algorithm previously proposed by Bell and Sejnowski (1995). According to figure 2, the input face images in X are considered to be a linear mixture of statistically independent basis images S combined by an unknown mixing matrix A. The ICA algorithm learns the weight matrix W, which is used to recover a set of independent basis images in the rows of U. In this architecture, the face images are variables, and the pixel values provide observations for the variables. The source separation, therefore, is performed in face space. Projecting the input images onto the learned weight vectors produces the independent basis images. The compressed representation of a face image is a vector of the coefficients used for linearly combining the independent basis images to generate the image.

The database of face images for training was organized into a matrix X where each row was a different image and the pixels were in columns, i.e., X had 200 rows (50 sheep × 4 face image per sheep) and 56000 columns (image resolution of 200 × 280). The number of ICs found by the ICA algorithm corresponds to the dimensionality of the input. As the training set consists of 200 images, the algorithm attempts to separate 200 ICs. In order to have control over the number of ICs extracted by the algorithm, ICA was not performed on the n original images but on a set of m linear combinations of those images, where $m < n$. To achieve this, principal component analysis (PCA; Turk and Pentland, 1991) was applied first to project the data into a subspace of dimension m to control the number of independent components produced by ICA. For these linear combinations, the first m principal component eigenvectors of the image set were chosen. The InfoMax algorithm was then applied to the eigenvectors to minimize the statistical dependence among resulting basis images. Liu and Weschler (1999) argued that pre-applying PCA enhances ICA performance by (1) discarding small trailing eigenvalues before whitening and (2) reducing computational complexity by minimizing pairwise dependencies. As PCA decorrelates the input data, and the remaining higher-order dependencies are separated by ICA.

The source images achieved by the rows of U are then used as basis images to represent faces. Face image representations consist of the coordinates of these images with respect to the image basis defined by the rows of U, and these coordinates are contained in the mixing matrix $A = W_I^{-1}$. W_Z is a whitening matrix defined by:

$$W_Z = 2 * \left[Cov(X)\right]^{-(1/2)} \tag{3}$$

Algorithm speed is increased by including a sphering step prior to learning. The sphering step removes the first- and second-order statistics of the data; both the mean and covariances are set to zero and the variances are equalized, which helps in speeding up the convergence of the ICA algorithm (Bell and Sejnowski, 1997). The row means of X are subtracted, and then X is passed through the whitening matrix W_Z. When the inputs to ICA are the sphered data, the full transform matrix W_I is the product of the sphering matrix and the matrix learned by ICA:

$$W_I = WW_Z \tag{4}$$

The weights W are updated according to the following learning rule:

$$W(t+1) = W(t) + \eta\ (I + Y'U^T)\ W \qquad (5)$$

where η is the learning rate, t is the time index, I is the identity matrix and Y' is the ratio between the second and first partial derivatives of the logistic function $f_i(U)$, which is define as:

$$f_i(U) = \frac{1}{1+e^{-U}} \qquad (6)$$

For further explanation on the derivation of equation 5, refer to Bell and Sejnowski (1995, 1997).

Let P_m denote the matrix containing the first m eigenvectors in its columns. The rows of the input matrix to ICA are variables and the columns are observations; therefore, ICA is performed on P_m^T, producing a matrix of m independent source images in the rows of U. The m independent basis images in the rows of U are computed as $U = W_I P_m^T$. Then, the coefficients b for the linear combination of basis images U that comprised the face images in X are determined as follows: Let R_m be the $n \times m$ matrix of PCA coefficients. Then:

$$R_m = XP_m \text{ and } X = R_m P_m^T \qquad (7)$$

From $U = W_I P_m^T$ and the assumption that W is invertible, we get:

$$P_m^T = W_I^{-1} U \qquad (8)$$

Therefore:

$$X = (R_m W_I^{-1})U = BU \qquad (9)$$

Hence, the rows of $R_m W_I^{-1} = B$ contained the coefficients for linearly combining the basis images to comprise the face image in the corresponding row of X.

The input matrix X was sphered according to equation 3, and the weights W were updated according to equations 5 and 6. After a few trials, it was observed that for high learning rates (such as 0.001), the algorithm became unstable, i.e., the weight changes became progressively larger. Proper convergence of the algorithm is marked by the weight changes decreasing progressively until a stable point is reached. Thus, the learning rate was initialized at 0.0004 and annealed down to 0.0001.

Face Recognition Performance

A representation for the test or verification images was obtained by using the PC representation based on the training images to obtain $R_{test} = X_{test} P_m$ and then computing:

$$B_{test} = R_{test} W_I^{-1} \qquad (10)$$

This was evaluated for the coefficient vectors b by the nearest-neighbor algorithm using cosines as the similarity measure. In each test set, the coefficient vectors were assigned the class label of the coefficient vector in the training set that was most similar, as evaluated by the cosine (c) of the angle between them:

$$c = \frac{b_{test} . b_{train}}{\|b_{test}\| \|b_{train}\|} \qquad (11)$$

The algorithm for image normalization and the face recognition algorithm by ICA were programmed in Matlab (version 7.14, The MathWorks Inc., Natick, Mass.).

Using four face images per sheep for the training stage, algorithm performance was tested for 200 IC (all possible IC), 180, 160, 140, 120, 100, 80, and 60 IC. Likewise, the recognition performance of the algorithm was assessed using a decreasing number of training images per animal. Training trials were performed using four face images per sheep (200 IC), three face images per sheep (150 IC), and two face images per sheep (100 IC). However, the number of images

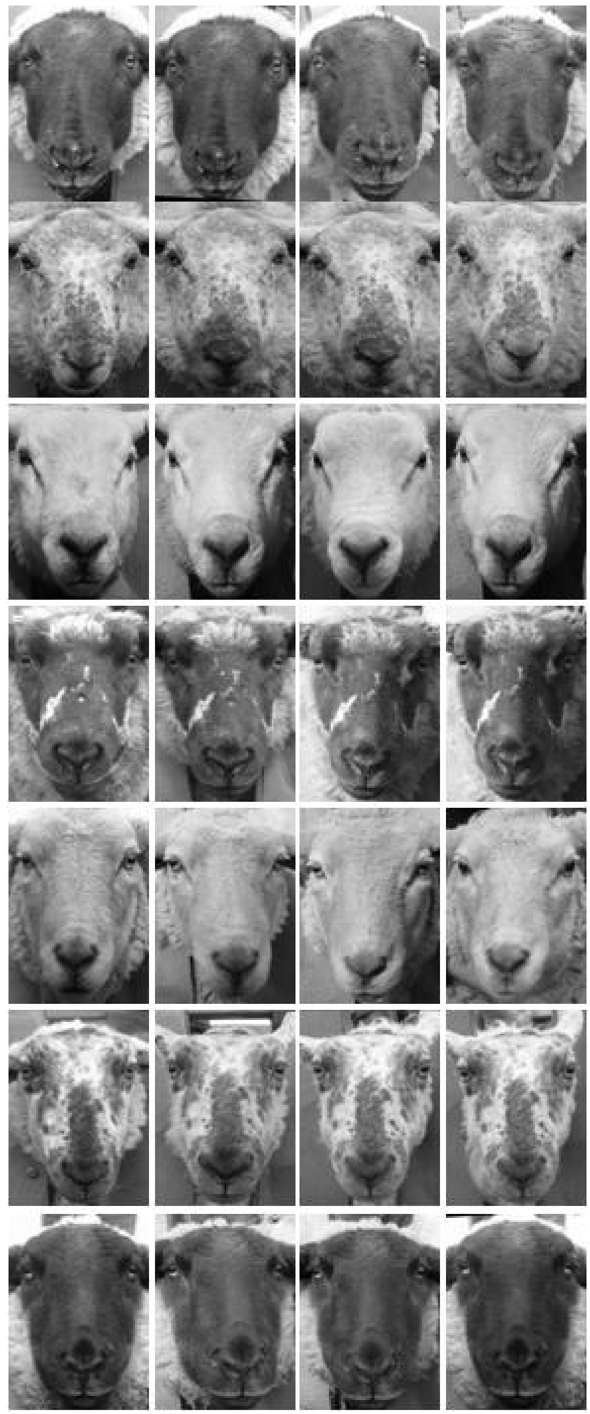

Figure 3. Samples of four-face image training sets of seven sheep acquired over a four-week period.

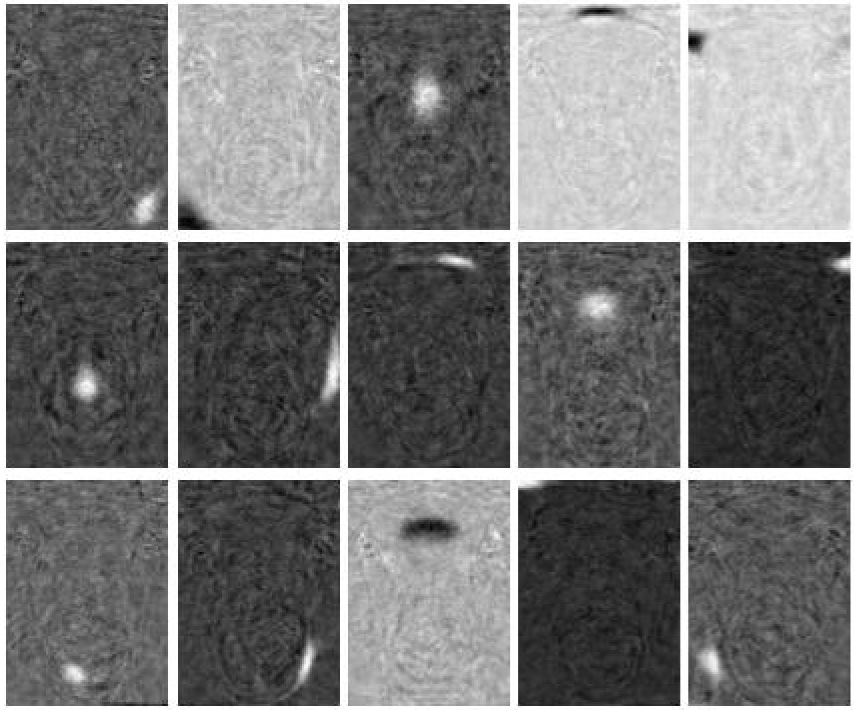

Figure 4. Fifteen statistically independent basis images reconstructed from the first 15 rows of matrix *U*.

per sheep (test images) for the verification stage remained constant for each trial (three face images per sheep).

Results and Discussion

The variability among face images of the same animal was mainly due to differences in pose and illumination. The degree of variability shown in figure 3, and similarly observed for the whole set of training images, was indeed desirable so as to assess the robustness of the independent component analysis technique for sheep face recognition. Some statistically independent basis images, reconstructed from the first 15 rows of *U*, are presented in figure 4. These basis images can be interpreted as follows: each row of the mixing matrix *W* represents a cluster of pixels that have similar behavior across images, and each row of the *U* matrix tells how close each pixel is to the cluster *i* identified by ICA. Since a sparse independent source model is used, these basis images are expected to be sparse and independent. The training and verification images are then considered to be linear combinations of these basis images (fig. 4) weighed with the coefficients (b_i) of the rows of the *B* matrix, i.e., $\sum b_n u_n$.

Using 200 and 180 ICs, the recognition rates were relatively high, reaching 96% and 95.3%, respectively (fig. 5). These rates were higher than those previously reported for human face recognition using ICA. Cheng et al. (2006) reported a recognition rate of 83% using this technique on a training set of 1000 front-view human facial images acquired under variable illumination and facial expression. With human face images taken on the same day but with different expressions, Bartlett et al. (2002) obtained a recognition rate of 88%. The fact that the facial expression of sheep is far more constant than that of human faces (fig. 3) could explain the higher recognition rates for sheep faces. However, when a lower number of ICs was selected (120 to 160), the recognition rate dropped to approximately 89.3% to 91.3% (fig. 5). A similar tendency was observed for the computational time. As a higher number of ICs was selected, the ICA representation was computationally more expensive (training time of 7 h for 200 IC and 3.5 h for 140 IC). On the contrary, the computational load decreased to ~18 min when the eigenfaces method (Turk and Pentland, 1991) was applied to a small set of 20 sheep faces (80 training images) retaining all eigenvectors (79). However, the mismatch error rate using the eigenfaces method was unacceptably high (30%), and for this reason, this method was not tested over the entire set of images.

In order to get an insight into the amount of within-class variability of the sheep face images, the ICA recognition performance was evaluated using a pooled approach of the cosine distance classifier when the 200 ICs were retained. For every test image, pooled cosine distances between the test

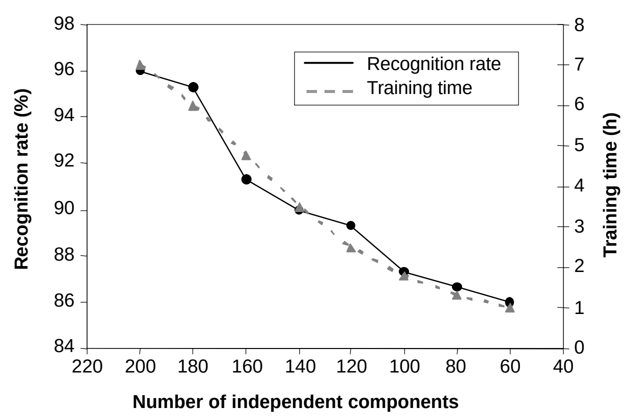

Figure 5. Influence of the number of independent components selected on recognition performance and training time.

image and the sheep face classes were calculated as Σcos (i), where i represents each of the four training images per sheep. So, for class label assignment of any test image, instead of finding the minimum value of 200 cosine distances, we found the minimum value of 50 pooled cosine distances. With this approach, 19 face images (out of 150) were misclassified, in contrast with the 6 face images misclassified when the ordinary cosine classifier was used. This indicates that the within-class variability is relatively high in relation to the between-class variability and should be reduced by standardizing the lighting conditions during imaging. We believe that the main factor inflating the within-class variability was the outdoor illumination, as it was variable and uncontrolled in this experiment, and to a lesser extent, differences in pose and possible facial distortions introduced by camera zooming (slightly wider or narrower faces). The histogram equalization in the image pre-processing step apparently did not sufficiently minimize the effects of variable illumination. More robust techniques for intensity normalization (Heseltine et al., 2002) should be evaluated.

A second experiment aimed to assess the influence of the number of training images per sheep on the recognition performance. In this case, the maximum number of ICs for four training images per sheep (200 IC), three training images per sheep (150 IC), and two training images per sheep (100 IC) were used. Recognition performance of each individual training set was evaluated on the 150 verification images. It is clear that an increase in the number of images per sheep for ICA training improved the recognition rate (fig. 6). The use of four and three training images per sheep produced recognition rates of 96% and 92%, respectively. However, when only two face images were used for algorithm training, the recognition rate dropped dramatically to 76%.

Beta distributions were fit to the histogram of the minimum cosine distance of image pairs originating from the same sheep (150 matching pairs) and to the histogram of cosine distance generated from image pairs of different sheep (2000 non-matching pairs) (fig. 7). As in any other biometric system, the main recognition errors, i.e., false match error (probability of mistaking two face images from different sheep to be from the same sheep) and false non-match error (probability of mistaking two face images from the same sheep to be from different sheep), arise from the overlap between these two distributions. Thus, whereas the cosine distance between matching images was found to be in the range [0.555 1.080], a small number of image pairs belonging to different sheep also fell into part of this range [0.800 1.080] (fig. 7). The errors associated with this biometric were estimated by defining a similarity score threshold or cutoff point. The classification rule using a similarity score threshold was as follows: a similarity score c was compared with an acceptance threshold c^*; if c was lower than or equal to c^*, then the compared face images were classified as belonging to the same animal. This classification rule originates two types of error, the false match error and the false non-match error, which were estimated from the fitted distributions (as outlined in Delac and Grgic, 2004).

The receiver operating characteristic (ROC) curve resulting from plotting false match error against false non-match error at different thresholds (fig. 8) represents a different decision strategy, i.e., the trade-offs that can be achieved between false match error and false non-match error. The overall performance of the face recognition system for sheep can then be judged by how bowed the ROC curve is. In an ideal biometric system, the ROC curve would be extremely bowed, reaching as far as possible into the lower left corner of figure 8, since reaching that limit would correspond to achieving a very high correct match rate (a very low false non-match rate) while keeping the false match rate at a very low value. The estimated cosine distance optimal threshold that minimizes the errors (see c^* at the intersection point between distributions in fig. 7) was 1.060 and produced a false match error of ~7.7% and a false non-match error of ~0.80%. The difference between the mismatch error (false match error) previously obtained from the verification image set (4%) and the false match error of ~7.7% estimated from the ROC curve occurs because, in the former case, the decision rule for matching was the minimum cosine distance while in the latter case, the decision rule for matching is based on the cosine distance threshold. While estimated error rates appeared to be relatively high using the cosine distance classifier, face recognition results reported by Draper et al. (2003) and Bartlett et al. (2002) showed that ICA had a better performance when the cosine similarity measure is used.

The cosine distances of the six false-match pairs of sheep images were 0.727, 0.854, 0.902, 0.947, 0.978, and 0.981, all within the range of cosine distance for matching images (two cases presented in fig. 9). For these false-match image pairs,

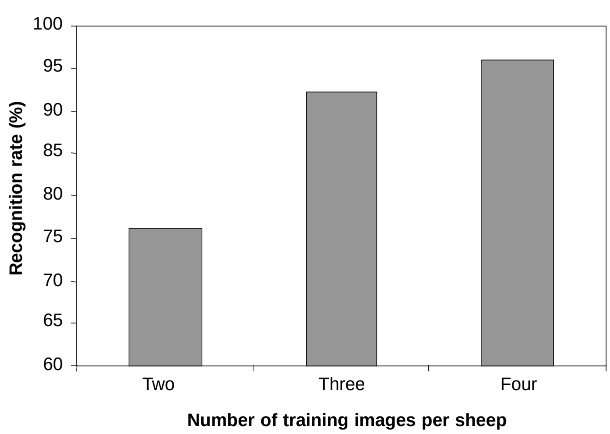

Figure 6. Sheep face recognition performance using two, three, and four images per sheep in the training set.

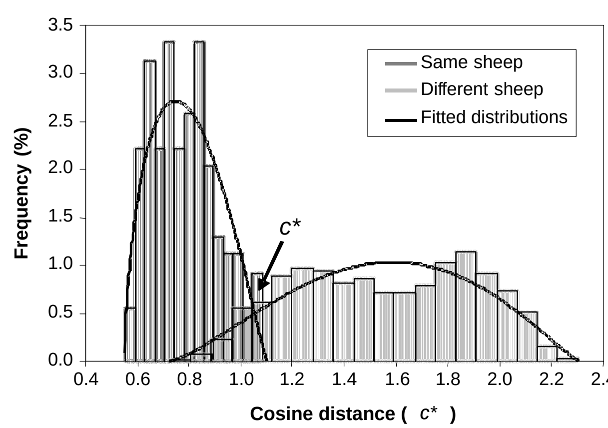

Figure 7. Distributions of cosine distance of image pairs from same sheep (minimum cosine distance, n = 150) and cosine distance of image pairs from different sheep (n = 2000).

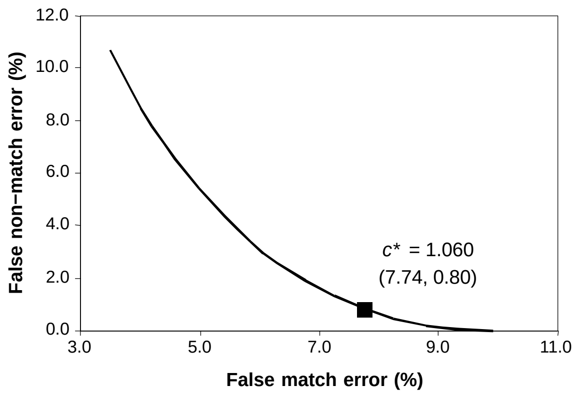

Figure 8. Receiver operating characteristic (ROC) curve showing cosine distance threshold (*c) that minimizes both false match error and false non-match error.**

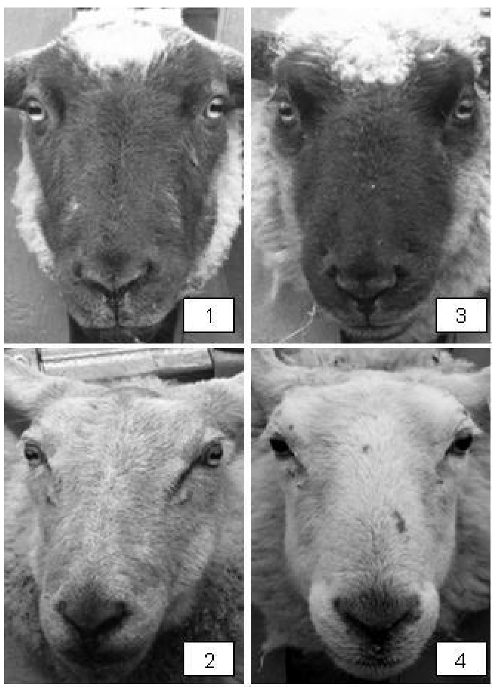

Figure 9. Two examples of face recognition failure when four face images were used for training. Sheep 3 and 4 (from the verification set of images) were misidentified as sheep 1 and 2 (from the training set of images).

Table 1. Some histogram features (mean, standard deviation, skewness, and kurtosis) and two features from the phase spectrum for the two false-match image pairs of figure 9.

Image Pair	Mean	SD	Skewness	Kurtosis	Laplacian 1	Laplacian 2
1	113.0	51.2	1.072	3.453	−11.79	−10.57
3	112.9	60.7	0.894	2.653	−13.10	−12.76
2	146.0	56.9	−0.335	1.845	−15.89	−13.92
4	142.9	59.5	−0.342	1.961	−16.94	−11.65

the minimum cosine distances were 0.981 and 0.902, respectively. Visual inspection of figure 9 shows that the false-match sheep were indeed very similar, which is also implied by the image statistics presented in table 1. Because the ICA technique is said to be sensitive to the phase spectrum of images, the Laplacians of the major peak phase (Laplacian 1) and the secondary peak phase (Laplacian 2) were included as additional comparative image features.

Although facial recognition as part of animal biometrics has not been investigated before, this preliminary work demonstrates that a subspace algorithm for human face recognition such as ICA performs well for sheep recognition. While far from being an automated system for sheep face recognition (i.e., sheep identification and verification), this work demonstrated the feasibility of performing such tasks with future refinement in terms of simpler image acquisition, higher recognition rates, and less computational expense. Further work is also needed to examine the impact of soil, residue, and long hair on the performance of sheep facial recognition.

Conclusions

One of the most popular approaches for human face recognition, independent component analysis with the cosine distance classifier, has been evaluated for sheep face recognition using a small set of normalized images. The results were very encouraging. Using all or most independent components (200 to 180), the recognition rate was as high as 95.3% to 96%. As expected, fewer independent components reduced the recognition rate, while a higher number of training images per sheep improved it. A classification criterion based on the cosine distance optimal threshold led to an estimated false match rate of 7.74% and an estimated false non-match rate of 0.80%. From this research, we can conclude that facial recognition, being non-invasive and inexpensive, is a potential biometric marker of sheep that could be used, initially, as means of verifying an animal's identity in any situation in which its identity is in doubt and, with further refinement of the technique, as a means of sheep identification. However, although the independent component analysis technique provided a reasonably good recognition performance (compared to human facial recognition), other recognition techniques should be assessed in order to improve accuracy by reducing the false match rate. It is recommended that the performance of other face recognition algorithms, such as linear discriminant analysis and support vector machines, be assessed on a very large set of sheep faces.

Acknowledgements

The authors wish to acknowledge that this research is supported by the Irish Government through the Department of Agriculture and Food under the National Development Plan 2000-2006.

References

Bartlett, M. S., J. R. Movellan, and T. J. Sejnowski. 2002. Face recognition by independent component analysis. *IEEE Trans. Neural Networks* 13(6): 1450-1463.

Bell, A. J., and T. J. Sejnowski. 1995. An information-maximization approach to blind separation and blind deconvolution. *Neural Comput*. 7(6): 1129-1159.

Bell, A. J., and T. J. Sejnowski. 1997. The independent components of natural scenes are edge filters. *Vision Res*. 37(23): 3327-3338.

Cardoso, J. F. 1997. Infomax and maximum likelihood for blind source separation. *IEEE Signal Processing Letters* 4(4): 112-114.

Cendrillón, P. 1999. Real-time face recognition using eigenfaces. BSc thesis. Brisbane, Australia: University of Queensland, Department of Computer Science and Electrical Engineering.

Cheng, J., Q. Liu, H. Lu, and Y. W. Chen. 2006. Ensemble learning for independent component analysis. *Pattern Recognition* 39(1): 81-88.

Delac, K., and M. Grgic. 2004. A survey of biometric recognition methods. In *Proc. 46th Intl. Symp. Electronics in Marine*. Zadar, Croatia: Croatian Society of Electronics in Marine.

De Luis García, R., C. Alberola López, O. Aghzout, and J. Ruiz Alzola. 2003. Biometric identification systems. *Signal Processing* 83(12): 2539-2557.

Draper, B. A., K. Back, M. S. Bartlett, and J. R. Beveridge. 2003. Recognizing faces with PCA and ICA. *Computer Vision and Image Understanding* 91(1-2): 115-137.

Dziuk, P. 2003. Positive, accurate animal identification. *Animal Reprod. Sci*. 79(3-4): 319-323.

Edwards, D. S., and A. M. Johnston 1999. Welfare implications of sheep ear tags. *Vet. Record* 144(22): 603-606.

Edwards, D. S., A. M. Johnston, and D. U. Pfeiffer. 2001. A comparison of commonly used ear tags on the ear damage of sheep. *Animal Welfare* 10: 141:151.

González, R. C., R. E. Woods, and S. L. Eddins. 2004. *Digital Image Processing Using Matlab*. Upper Saddle River, N.J.: Pearson Prentice Hall.

Heseltine, T., N. Pears, and J. Austin. 2002. Evaluation of image pre-processing techniques for eigenface-based face recognition. In *Proc. 2nd Intl. Conf. Image and Graphics*, 677-685. Bellingham, Wash.: SPIE. Available at: www.cs.york.ac.uk/~tomh. Accessed 23 January 2006.

Jiménez Gamero, I., G. Dorado, A. Muñoz Serrano, M. Analla, and A. Alonso Moraga. 2006. DNA microsatellites to ascertain pedigree-recorded information in a selecting nucleus of Murciano-Granadina dairy goats. *Small Ruminant Res.* 65(3): 266-273.

Liu, C., and H. Weschler. 1999. Comparative assessment of independent component analysis (ICA) for face recognition. In *Proc. 2nd Intl. Conf. Audio and Video Based Biometric Person Authentication*, 211-216. Washington, D. C. Available at: www.face-rec.org/algorithms/ICA/liu99comparative.pdf.

Loftus, R. 2005. Traceability of biotech-derived animals: application of DNA technology. *Rev. Sci. Tech. Off. Int. Epiz.* 24(1): 231-242.

Moon, H., and P. J. Phillips. 2001. Computational and performance aspects of PCA-based face recognition algorithms. *Perception* 30(3): 303-321.

Raschke, A., S. Strich, S. Huppke, M. Neugebauer, E. Geuther, W. Bertling, B. Walders, C. Reiser, and J. Hess. 2006. Induction and detection of long-lasting peptide-specific antibody responses in pigs and beef cattle: A powerful technology for tracing meat processing chains from stock farmers to sales counters. *Food Control* 17(1): 65-74.

Rusk, C. P., Blomeke, C. R., Balschweid, M. A., Elliot, S. J., and Baker, D. 2006. An evaluation of retinal imaging technology for 4-H beef and sheep identification. *J. Extension* 44(5). Available at: www.joe.org/joe/2006october/a7.shtml.

Shakhnarovich, G., and B. Moghaddam. 2004. Face recognition in subspaces. In *Handbook of Face Recognition*, 141-168. S. Z. Li and A. K. Jain, eds. New York, N.Y.: Springer Verlag.

Smith, G. C., J. D. Tatum, K. E. Belk, J. A. Scanga, T. Grandin, and J. N. Sofos. 2005. Traceability from a U.S. perspective. *Meat Sci.* 71(1): 174-193.

Turk, M., and A. Pentland. 1991. Eigenfaces for recognition. *J. Cognitive Neurosci.* 3(1): 71-86.

Yuen, P. C., and J. H. Lai. 2002. Face representation using independent component analysis. *Pattern Recognition* 35(6): 1247-1257.